

Accurate sensorless displacement control based on the electrical resistance of the shape memory actuator

Journal of Intelligent Material Systems and Structures
2023, Vol. 34(9) 1097–1103
© The Author(s) 2022
Article reuse guidelines:
sagepub.com/journals-permissions
DOI: 10.1177/1045389X221128568
journals.sagepub.com/home/jim



Ali Berhil^{1,2}, Mahmoud Barati^{1,2,3}, Yves Bernard^{1,2}
and Laurent Daniel^{1,2}

Abstract

This paper aims to implement the controllable deformation of a structure using Shape Memory Alloys (SMA) actuators. A sensorless displacement estimation method is proposed. This method is tested on a prototype composed of a disc, beams, and SMA actuators. By measuring the variation of electrical resistivity in SMA springs, as a feedback signal in the closed-loop position control, the surface displacement is obtained without any external displacement sensor. The proposed method is validated by comparing the displacement values estimated by the electrical resistivity measurement with those measured by a laser sensor. The estimated displacement and the measured displacement follow the reference displacement with steady-state errors, respectively of 1.14% and 0.42%.

Keywords

Shape memory actuator, morphing structure, displacement control, self-sensing, electrical resistance feedback

1. Introduction

The use of morphing structures is growing significantly. In aeronautics and wind turbine blade applications, morphing structures bring significant improvement in aerodynamic performance. In aeronautics, this concept is adopted to enhance aerodynamic performance by continuously varying the wings geometry during flight through the control of Shape Memory Alloys (SMA) components (Scherer et al., 1999; Simiriotis, 2021). In addition, to improve efficiency, the use of morphing actuators based on SMA actuators allows to reduce drag, save fuel, and promote the design of lightweight structures.

Shape Memory Alloys are smart materials that can be used as actuators and integrated into structures. The SMA activation allows modifying the shape of the structure in which it is embedded (Basit et al., 2013; Hussein et al., 2016; Kang et al., 2012; Naghashian et al., 2014). SMA actuators are characterized by very high energy density, silent operation, and self-sensing capability (Dhanalakshmi, 2013; Lan and Fan, 2010). SMA actuators can be divided into two types: one-way SMA actuators and two-way SMA actuators. A one-way SMA actuator needs an external force to be applied during the cooling phase to allow cyclic

actuation. A two-way SMA actuator can produce a cyclic actuation without the need for an external force. In this research, a prototype is developed in order to implement a morphing structure with pre-stressed one-way SMA actuators. The required external force is applied by the structure to be deformed.

Actuators based on SMAs have excellent potential in applications where weight, space, and noise are crucial factors, as in aerospace applications, robotic manipulations, and micro-manufacturing (Kohl, 2018). Several applications can be cited, for instance, SMA human hand development (Simone et al., 2017) or reconfigurable aircraft wings (Strelec et al., 2003). SMA actuators can produce force to deform the structure in which they are inserted when heated. This heating can be obtained

¹CentraleSupélec, CNRS, Laboratoire de Génie Electrique et Electronique de Paris, Université Paris-Saclay, Gif-sur-Yvette, France

²CNRS, Laboratoire de Génie Electrique et Electronique de Paris, Sorbonne Université, Paris, France

³Institut Polytechnique des Sciences Avancées, IPSA, Ivry-sur-Seine, France

Corresponding author:

Laurent Daniel, GeePs-CentraleSupélec, 3 Rue Joliot Curie, Gif-sur-Yvette, 91192, France.

Email: laurent.daniel@centralesupelec.fr



Figure 1. Experimental setup.

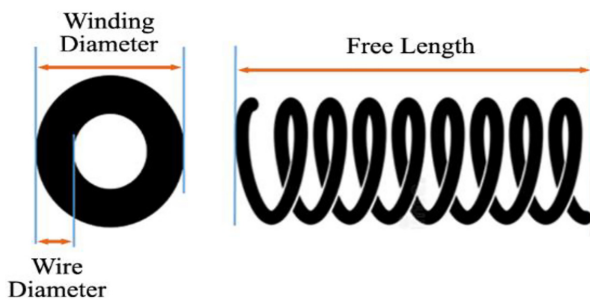


Figure 2. Illustration of the SMA spring parameters and corresponding characteristics.

Table 1. SMA spring parameters.

Winding diameter (mm)	Spring wire diameter (mm)	Free length of the spring (mm)	Transformation temperatures
6	0.75	20	$A_f = 44^\circ\text{C}$ $A_s = 33^\circ\text{C}$ $M_f = 28^\circ\text{C}$ $M_s = 21^\circ\text{C}$

by Joule effect. SMA actuators recover considerable strains up to 8% (Eschen and Abel, 2018).

There are different methods to control SMA actuators using an external displacement sensor (Dominik, 2016; Kha and Ahn, 2006; Moallem and Tabrizi, 2008; Song, 2002; Troisfontaine et al., 1998). Direct control with the use of a displacement laser sensor is presented in Song et al. (2000), control with the use of temperature as a feedback signal in Troisfontaine et al. (1998), and indirect control displacement based on the SMA electrical resistance as a feedback signal in the control loop in Raparelli et al. (2002), Lan and Fan (2010), Malukhin and Ehmann (2008), Liu et al. (2010), and Takeda et al. (2008).

The use of electrical resistance (E.R.) as a sensor is investigated in a few references (Karimi and Konh, 2020; Precht et al., 2020; Sarmento et al., 2022;

Simone et al., 2017; Urata et al., 2007). These studies focus on a SMA that undergoes a constant stress value. SMA electrical resistivity is affected by several factors such as stress, deformation, temperature, and phase transformation (Barati et al., 2017; Nakshatharan and Dhanalakshmi, 2014; Novák et al., 2008; Rączka et al., 2013; Raparelli et al., 2002; Sławski et al., 2021). The models representing the relationship between the SMA electrical resistance and SMA displacement are presented in Kumar and Lagoudas (2008), Lynch et al. (2016), and Dutta Ghorbel (2005).

In the case studied in the present paper, the applied stress and strain are variable at the same time.

In this paper, different control techniques for SMA actuators are implemented experimentally. The first one is based on a position feedback control with a PID controller. An accurate displacement control is demonstrated through step response and sinusoidal tracking. The second one is based on the SMA electrical resistance feedback to estimate the structure displacement. The goal is to eliminate the need for a position sensor.

Section 2 describes the experimental setup and the structure on which the shape morphing is implemented. The implementation of PID control displacement of the studied structure using laser sensor displacement is presented in section 3. Section 4 shows the implementation and validation of a sensorless control loop displacement based on the SMA electrical resistance measurement.

2. Studied morphing structure

The studied structure is composed of a disc with four external beams and one central beam. The SMA actuators are connected between an external beam EB and the central one CB (see Figure 1). SMA spring actuators are used in our prototype. The constitutive model and position control of the shape memory alloy spring are presented in Hu et al. (2022). The characteristics of the SMA spring actuator are given in Figure 2 and Table 1.

The SMA springs are pre-strained before being mounted into the prototype. The amplitude of the electric current in the SMA springs is set by the control system. The temperatures of the martensitic transformation of the SMA actuators should be chosen according to the climatic conditions of the geographical area where they will be used.

The connection between the structure and the SMA actuators is made through cylindrical beams. The height of the beams allows to set the stiffness of the structure. The illustration of the complete experimental setup is shown in Figure 3.

The displacement reference signal is given via a graphical interface developed under the ControlDesk software. The displacement of the disc is obtained from a

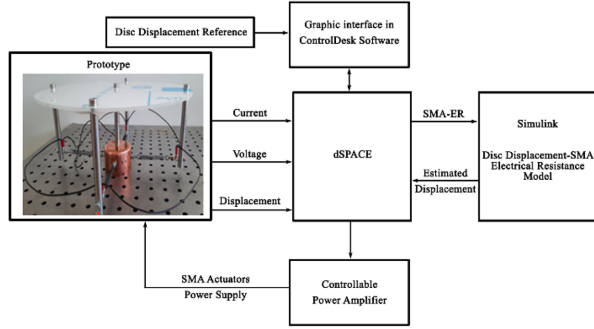


Figure 3. Illustration of the experimental setup.

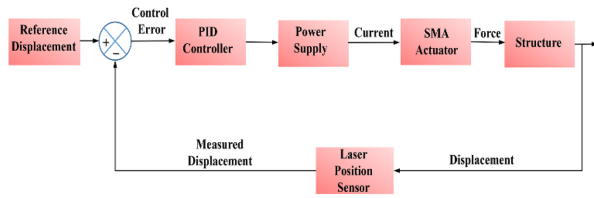


Figure 4. General principle of the control system for structure displacement with SMA actuators.

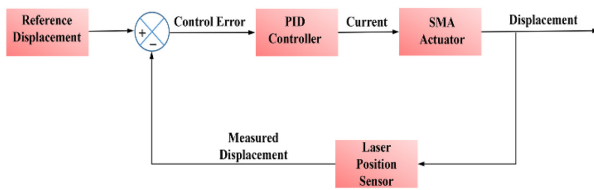


Figure 5. Block diagrams for control loop displacement: PID regulator.

laser sensor KEYENCE LK-G152. The displacement is acquired through the Analog Digital Converter (ADC) of the dSPACE control card. The electric current and voltage of the SMA actuators are measured in order to deduce the SMA electrical resistance. The SMA spring actuators are connected and supplied in parallel. The

positive terminal of the power supply is connected to one of the external beams, and the negative terminal of the power supply is connected to the central beam. The entire control hardware size can be minimized if a micro-controller is used (Sreekanth et al., 2018).

3. PID position control loop

This section presents the implementation results of a structure displacement closed-loop (see Figures 4 and 5). A classical position PID control loop is considered.

The PID regulator is synthesized in order to address the following specifications: no overshoot of the reference value, steady-state error less than 1.2%, and response time of 1 s to reach 95% of the reference value.

The response time at 5% of the system in order to follow a new reference (e.g., to move from 0.5 to 0.6 mm) is equal to 1 s. The steady-state displacement error is 0.42%. Figure 6 shows that the PID controller is able to follow a successive step and sine wave displacement reference in the absence of disturbance. The PID controller has been synthesized to have no overshoot, which is verified in Figure 6. The implemented PID regulator respects the controller specifications.

4. Control loop displacement with electrical resistivity measurement

The purpose of this part is to control the structure displacement by measuring the electrical resistance of the SMA, avoiding the laser displacement sensor as in the previous part. The determination of the relationship between the structure displacement and the SMA electrical resistance (as is shown later in Figure 9) allows predicting the position of the structure without a position sensor. A displacement control loop using the measurement of the SMA electrical resistance as a feedback signal is implemented experimentally. The block diagram of this loop is shown in Figure 7.

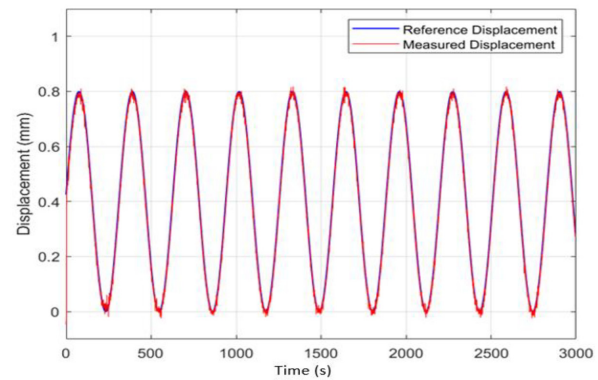
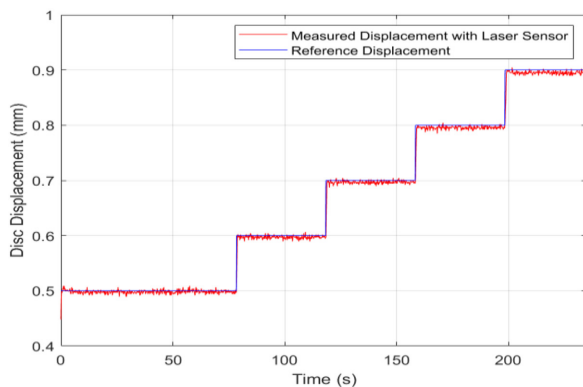


Figure 6. Reference and measured disc displacement with PID controller: step (left) and sine (right) reference signals.

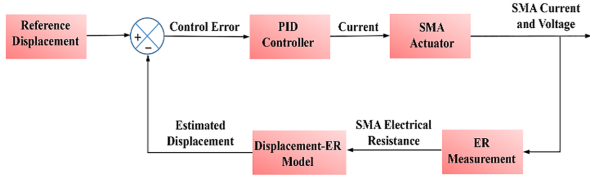


Figure 7. Displacement control loop using the SMA electrical resistance measurement.

In order to establish the relationship between resistance and displacement, the disc displacement is plotted as a function of the SMA electrical current and voltage (Figure 8).

At the starting point (point A in Figure 8), before heating, the displacement of the disk is zero. By increasing the electric current, the SMA component heats up, and this leads to the deformation of the structure and consequently to the displacement of the disk along the Z-axis. At the end of the heating (point B in Figure 8), the disc displacement is about 1.1 mm. During cooling, the disc returns to its initial position with zero displacements (point A in Figure 8). Figure 8 shows the hysteric behavior of the structure displacement as a function of the electric current through the SMA actuator (left) and as a function of the SMA electric voltage.

Figure 9 shows the variation of the disc displacement as a function of the electrical resistance of the shape memory alloy, deduced from the results of Figure 8. A small hysteresis between heating and cooling is observed. This curve is used to estimate the displacement without using the laser sensor.

Using curve fitting tools in MATLAB, the curve of Figure 9 is fitted. The goal is to find the mathematical model that will be implemented in the control loop of Figure 7. A polynomial function at the order six is chosen (see equation (1)). DH is the disc displacement during the heating cycle. R represents the SMA electrical

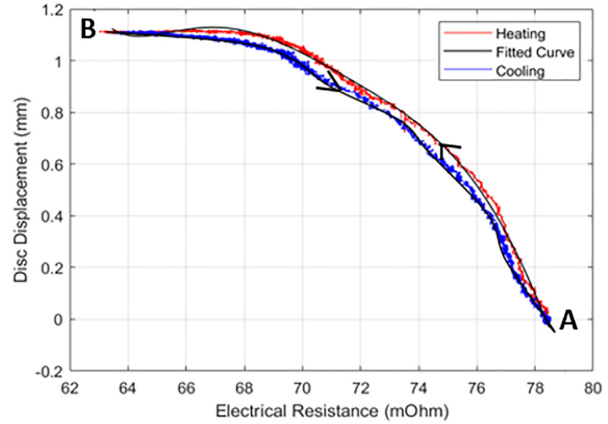


Figure 9. Disc displacement versus SMA electrical resistance.

resistance in the heating phase. The coefficients of equation (1) are given in Table 2.

$$DH = p1.R^5 + p2.R^4 + p3.R^3 + p4.R^2 + p5.R + p6 \quad (1)$$

Similarly, the equation for the relationship between displacement and electrical resistance during the cooling part is given by equation (2). DC is the disc displacement in the cooling phase. R represents the SMA electrical resistance in the cooling phase. The coefficients of equation (2) are given in Table 3.

$$DC = q1.R^4 + q2.R^3 + q3.R^2 + q4.R + q5 \quad (2)$$

Equations (1) and (2) are implemented into the displacement control loop. Experimental tests are conducted on the prototype to evaluate the validity and performance of the SMA displacement control using electrical resistance.

Figure 10 illustrates the real-time estimated displacement using the SMA electrical resistance measurement for a continuous step reference. It is observed that the

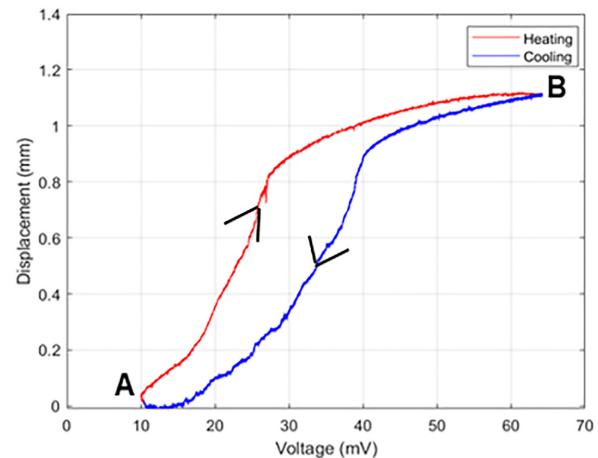
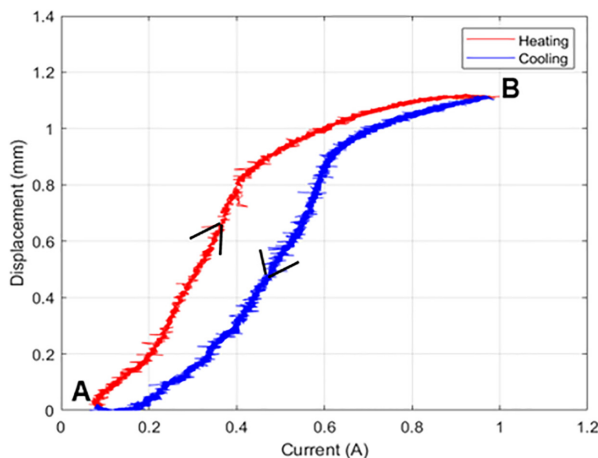


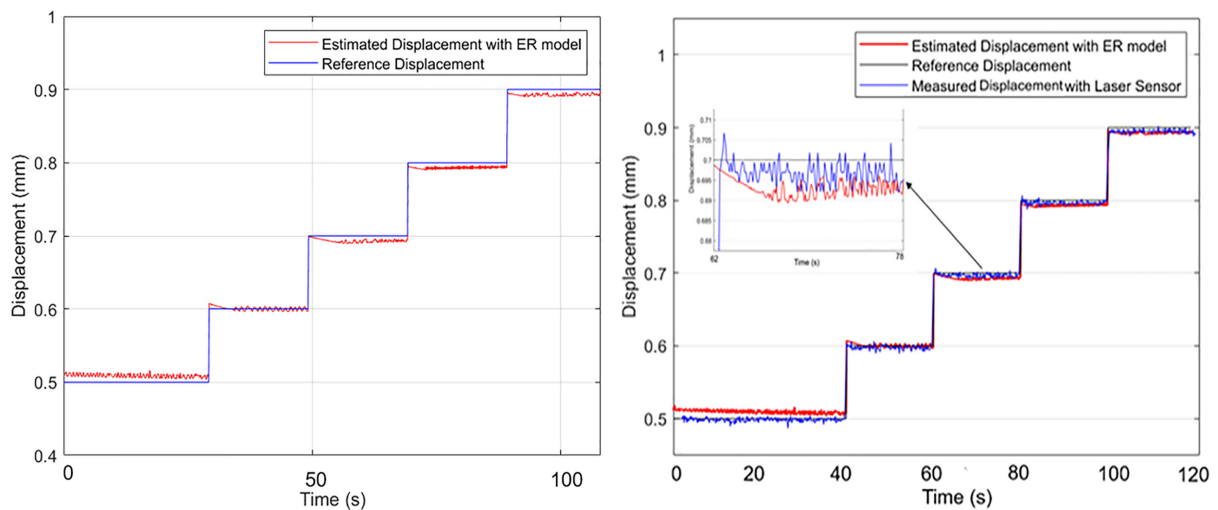
Figure 8. Disc displacement versus SMA electrical current (left) and voltage (right).

Table 2. Coefficients of the polynomial function for the heating phase.

p_1	p_2	p_3	p_4	p_5	p_6
$-1.2 \cdot 10^{-5} \text{ m}/\Omega^5$	$4.0 \cdot 10^{-3} \text{ m}/\Omega^4$	$-5.7 \cdot 10^{-1} \text{ m}/\Omega^3$	$4.0 \cdot 10^1 \text{ m}/\Omega^2$	$-1.4 \text{ m}/\Omega$	1.9 m

Table 3. Coefficients of the polynomial function for the cooling phase.

q_1	q_2	q_3	q_4	q_5
$-2.0 \cdot 10^{-5} \text{ m}/\Omega^4$	$5.0 \cdot 10^{-3} \text{ m}/\Omega^3$	$-5.3 \cdot 10^{-1} \text{ m}/\Omega^2$	$2.4 \cdot 10^1 \text{ m}/\Omega$	-4.1 m

**Figure 10.** Reference and estimated disc displacement with electrical resistance model.

estimated displacement matches with the displacement reference with a steady-state error displacement of 1.14%. To validate this control loop, the disc displacement obtained with the laser sensor and the estimated displacement with the same reference are compared. Figure 10 shows that the estimated displacement and the measured displacement follow the reference displacement with steady-state errors, respectively of 1.14% and 0.42%.

5. Conclusion

A mechanical structure composed of a disc and five cylindrical beams actuated by four SMA springs is used to demonstrate the implementation of a controlled deformable surface. Two control techniques are investigated and implemented to control the structure displacement. The first one is a classical PID position control. The second one is based on the use of SMA electrical resistance as the feedback signal. To implement this latter control, the relationship between the disc displacement and the SMA electrical resistance is identified experimentally and used as a self-sensing feature. This

relationship is integrated into the global control loop to predict the disc displacement without an external sensor. The control loop is implemented for the control of displacement values in the order of 1 mm. The control loop with laser displacement has an excellent time response performance and a slightly better steady-state error (0.42%) compared to the sensorless approach (1.14%). The real-time sensorless control system using the electrical resistance of the SMA actuators as the feedback signal is implemented and validated. This control system is applied to a morphing structure in order to control the surface shape of the developed prototype.

Declaration of conflicting interests

The author(s) declared no potential conflicts of interest with respect to the research, authorship, and/or publication of this article.


Funding


The author(s) disclosed receipt of the following financial support for the research, authorship, and/or publication of

this article: The authors acknowledge the support of the French Agence Nationale de la Recherche (ANR), under grant ANR-16-CE08-0011 (project ETAE).

ORCID iDs

Ali Berhil  <https://orcid.org/0000-0002-6554-6093>

Mahmoud Barati  <https://orcid.org/0000-0003-1928-929X>

Laurent Daniel  <https://orcid.org/0000-0001-5016-4589>

References

- Barati M, Chirani SA, Kadhodaei M, et al. (2017) On the origin of residual strain in shape memory alloys: Experimental investigation on evolutions in the microstructure of CuAlBe during complex thermomechanical loadings. *Smart Materials and Structures* 26(2): 025024.
- Basit A, L'Hostis G and Durand B (2013) High actuation properties of shape memory polymer composite actuator. *Smart Materials and Structures* 22(2): 025023.
- Dhanalakshmi K (2013) Demonstration of self-sensing in shape memory alloy actuated gripper. In: *IEEE International Symposium on Intelligent Control (ISIC)*, Hyderabad, India, 28–30 August, pp.218–222.
- Dominik I (2016) Type-2 fuzzy logic controller for position control of shape memory alloy wire actuator. *Journal of Intelligent Material Systems and Structures* 27(14): 1917–1926.
- Dutta SM and Ghorbel FH (2005) Differential hysteresis modeling of a shape memory alloy wire actuator. *IEEE/ASME Transactions on Mechatronics* 10(2): 189–197.
- Eschen K and Abel J (2018) Performance and prediction of large deformation contractile shape memory alloy knitted actuators. *Smart Materials and Structures* 28(2): 025014.
- Hu B, Liu F, Mao B, et al. (2022) Modeling and position control simulation research on shape memory alloy spring actuator. *Micromachines* 13(2): 178.
- Hussein AMH, Majid DA and Abdullah EJ (2016) Shape memory alloy actuation effect on subsonic static aeroelastic deformation of composite cantilever plate. *IOP Conference Series: Materials Science and Engineering* 152(1): 012010.
- Kang TH, Lee JM, Yu WR, et al. (2012) Two-way actuation behavior of shape memory polymer/elastomer core/shell composites. *Smart Materials and Structures* 21(3): 035028.
- Karimi S and Konh B (2020) Self-sensing feedback control of multiple interacting shape memory alloy actuators in a 3D steerable active needle. *Journal of Intelligent Material Systems and Structures* 31(12): 1524–1540.
- Kha NB and Ahn KK (2006) Position control of shape memory alloy actuators by using self tuning fuzzy PID controller. In: *1ST IEEE conference on industrial electronics and applications*, Singapore, 24–26 May 2006, pp.1–5. New York, NY: IEEE.
- Kohl M, Fechner R, Gueltig M, et al. (2018) Miniaturization of shape memory actuators. In: *ACTUATOR 2018, 16th international conference on new actuators*, Bremen, Germany, 25–27 June 2018, pp.1–9. New York, NY: IEEE.
- Kumar PK and Lagoudas DC (2008) Introduction to shape memory alloys. In: Lagoudas DC (ed.) *Shape Memory Alloys*. Boston, MA: Springer, pp.1–51.
- Lan CC and Fan CH (2010) An accurate self-sensing method for the control of shape memory alloy actuated flexures. *Sensors and Actuators A: Physical* 163(1): 323–332.
- Liu SH, Huang TS and Yen JY (2010) Tracking control of shape-memory-alloy actuators based on self-sensing feedback and inverse hysteresis compensation. *Sensors* 10(1): 112–127.
- Lynch B, Jiang XX, Ellery A, et al. (2016) Characterization, modeling, and control of Ni-Ti shape memory alloy based on electrical resistance feedback. *Journal of Intelligent Material Systems and Structures* 27(18): 2489–2507.
- Malukhin K and Ehmann KF (2008) An experimental investigation of the feasibility of “self-sensing” shape memory alloy based actuators. *Journal of Manufacturing Science and Engineering* 130(3): 031109.
- Moallem M and Tabrizi VA (2008) Tracking control of an antagonistic shape memory alloy actuator pair. *IEEE Transactions on Control Systems Technology* 17(1): 184–190.
- Naghashian S, Fox BL and Barnett MR (2014) Actuation curvature limits for a composite beam with embedded shape memory alloy wires. *Smart Materials and Structures* 23(6): 065002.
- Nakshatharan S and Dhanalakshmi K (2014) Differential resistance feedback control of a self-sensing shape memory alloy actuated system. *ISA Transactions* 53(2): 289–297.
- Novák V, Šittner P, Dayananda GN, et al. (2008) Electric resistance variation of NiTi shape memory alloy wires in thermomechanical tests: Experiments and simulation. *Materials Science and Engineering: A* 481: 127–133.
- Precht J, Seelecke S, Motzki P, et al. (2020) Self-sensing control of antagonistic SMA actuators based on resistance-displacement hysteresis compensation. *Smart Materials, Adaptive Structures and Intelligent Systems* 84027: V001T03A001.
- Rączka W, Konieczny J and Sibielski M (2013) Laboratory tests of shape memory alloy wires. *Solid State Phenomena* 199: 365–370.
- Raparelli T, Zobel PB and Durante F (2002) SMA wire position control with electrical resistance feedback. In: *Proceedings of 3rd world conference on structural control*, Como, Italy, April 7 2002, Vol. 2, pp.391–398.
- Sarmiento NL, Basilio JM, Cunha MF, et al. (2022) Force control of a shape memory alloy spring actuator based on internal electric resistance feedback and artificial neural networks. *Applied Artificial Intelligence* 36: 2015106.
- Scherer LB, Martin CA, West MN, et al. (1999) DARPA/ARFL/NASA smart wing second wind tunnel test results. *Smart Structures and Materials* 1999: Industrial and Commercial Applications of Smart Structures Technologies 3674: 249–259.
- Simiriotis N, Fragiadakis M, Rouchon JF, et al. (2021) Shape control and design of aeronautical configurations using shape memory alloy actuators. *Computers & Structures* 244: 106434.
- Simone F, Rizzello G and Seelecke S (2017) Metal muscles and nerves: A self-sensing SMA-actuated hand concept. *Smart Materials and Structures* 26(9): 095007.
- Slawski S, Kciuk M and Klein W (2021) Assessment of SMA electrical resistance change during cyclic stretching with small elongation. *Sensors* 21(20): 6804.

- Song G (2002) Robust position regulation of a shape memory alloy wire actuator. *Proceedings of the Institution of Mechanical Engineers, Part I: Journal of Systems and Control Engineering* 216(3): 301–308.
- Song G, Lam PC, Srivatsan TS, et al. (2000) Application of shape memory alloy wire actuator for precision position control of a composite beam. *Journal of Materials Engineering and Performance* 9(3): 330–333.
- Sreekanth M, Mathew AT and Vijayakumar R (2018) A novel model-based approach for resistance estimation using rise time and sensorless position control of sub-millimetre shape memory alloy helical spring actuator. *Journal of Intelligent Material Systems and Structures* 29(6): 1050–1064.
- Strelec JK, Lagoudas DC, Khan MA, et al. (2003) Design and implementation of a shape memory alloy actuated reconfigurable airfoil. *Journal of Intelligent Material Systems and Structures* 14(4–5): 257–273.
- Takeda Y, Cho H, Yamamoto T, et al. (2008) Control characteristics of shape memory alloy actuator using resistance feedback control method. *Advances in Science and Technology* 59: 178–183.
- Troisfontaine N, Bidaud P and Dario P (1998) Control experiments on two SMA based micro-actuators. In: Casals A and de Almeida AT (eds) *Experimental Robotics V*. Berlin, Heidelberg: Springer, pp.490–499.
- Urata J, Yoshikai T, Mizuuchi I, et al. (2007) Design of high DOF mobile micro robot using electrical resistance control of shape memory alloy. In: *IEEE/RSJ International Conference on Intelligent Robots and Systems, San Diego, CA, 29 October–2 November*, pp.3828–3833. New York, NY: IEEE.